Cardiovascular Toxicology (2019) 19:264–275
https://doi.org/10.1007/s12012-018-9495-6

MiR-15b-5p is Involved in Doxorubicin-Induced Cardiotoxicity via Inhibiting Bmpr1a Signal in H9c2 Cardiomyocyte

Guo-xing Wan[1] · Lan Cheng[1] · Hai-lun Qin[1] · Yun-zhang Zhang[1] · Ling-yu Wang[1] · Yong-gang Zhang[1]

Published online: 7 December 2018

Abstract
The wide use of anthracyclines represented by doxorubicin (DOX) has benefited cancer patients, yet the clinical application is limited due to its cardiotoxicity. Although numerous evidences have supported a role of microRNAs (miRNAs) in DOX-induced myocardial damage, the exact etiology and pathogenesis remain largely obscure. In this study, we focused on the role of miR-15b-5p in DOX-induced cardiotoxicity. We employed a public miRNA and gene microarray to screen differentially expressed miRNAs (DEMs) and differentially expressed genes (DEGs) in rat cardiomyocytes, and 33 DEMs including miR-15b-5p and 237 DEGs including Bmpr1a and Gata4 were identified. The Gene ontology (GO) and pathway enrichment analysis of 237 DEGs indicated that the DEGs were mainly enriched in heart development and ALK pathway in cardiomyocyte which included the main receptor Bmpr1a and transcription factor Gata4. The up-regulated miR-15b-5p and down-regulated Bmpr1a and Gata4 mRNA expressions were further validated in H9c2 cardiomyocytes exposed to DOX. Moreover, the results showed overexpression of miR-15b-5p or inhibition of Bmpr1a may enhance the DOX-induced apoptosis, oxidative stress and mitochondria damage in H9c2 cardiomyocytes. The Bmpr1a was suggested as a potential target of miR-15b-5p by bioinformatics prediction. We further verified the negatively regulatory effect of miR-15b-5p on Bmpr1a signaling. Moreover, we also confirmed that overexpression of miR-15b-5p may exacerbate the DOX-induced apoptosis of H9c2 cardiomyocytes by affecting the protein expression ratio of Bcl-2/Bax and Akt activation, while this pro-apoptotic effect was able to be suppressed by Bmpr1a agonist. Collectively, the results suggest that miR-15b-5p is likely involved in doxorubicin-induced cardiotoxicity via inhibiting Bmpr1a signaling in H9c2 cardiomyocytes. Our study provides a novel insight for investigating DOX-induced cardiotoxicity.

Keywords MiR-15b-5p · Bmpr1a · Doxorubicin · Cardiotoxicity

Introduction

Doxorubicin (DOX) is one of the most widely used and forceful anthracycline agents, delivering anti-cancer activity against numerous types of malignancy. However, the clinical benefit of DOX treatment has been limited by its cumulative and dose-dependent cardiotoxicity [1]. With an accumulation dose of DOX increased from 400 to 700 mg/m^2, the incidence of heart failure or left ventricular dysfunction rises from 5 to 48% [2], which may impair the survival benefit DOX treatment brings. Current evidences have proposed several mechanisms accounting for DOX-induced cardiotoxicity, including oxidative stress, inflammation, lipid peroxidation, mitochondrial impairment, intracellular calcium dysregulation and inhibitory topoisomerase II (Top2), which may be involved in irreversible myocardial damage and apoptosis [3–5]. Nevertheless, the exact mechanisms remain poorly understood.

MicroRNAs (miRNAs) as key players in gene expression regulation by altering the translation or stability of target mRNAs have been found functionally participated in heart development, function, and diseases including DOX-induced cardiotoxicity [6]. Recently, miR-15b was found up-regulated in the mice ischemia reperfusion (I/R) model [7]. Similarly, miR-15b was also reported to enhance hypoxia/

Handling Editor: Gen Suzuki.

✉ Yong-gang Zhang
zhangyg8686@hotmail.com

[1] Department of Cardiology, The Second Affiliated Hospital of Shantou University Medical College, Dongxia North Road, Shantou 515041, Guangdong, People's Republic of China

reoxygenation (H/R)-induced apoptosis of cardiomyocytes via a mitochondrial apoptotic pathway [8]. Conversely, the suppression of miR-15b was able to prevent rapid loss of cardiac function in an induced cardiac dysfunction model in adult mice [9]. Moreover, the inhibition of miR-15b was found capable of decreasing apoptosis in neonatal rat cardiac myocytes by modulating cellular adenosine triphosphate (ATP) level and mitochondrial integrity [10]. Consequently, the current findings suggested that the manipulation of miR-15b was likely developed for therapeutic approaches [9]. However, the role of miR-15b in DOX-induced cardiotoxicity remains largely unknown.

In this study, the differentially expressed miRNAs in DOX-treated cardiomyocytes were identified by using a public microarray dataset. We focused on the role of miR-15b in the cardiomyocytes exposed to DOX, and explored the underlying mechanism, which may provide a valuable insight to protect against DOX-induced cardiotoxicity.

Materials and Methods

Chemicals and Materials

DOX was obtained from Hisun-Pfizer Pharmaceutical Co., Ltd. (Zhejiang, China), which was dissolved in PBS. Protein Extraction Kit was obtained from KEYGEN Biotech. Co., Ltd. (Nanjing, China). The ROS assay kit, mitochondrial membrane potential assay kit with JC-1, cell lysis buffer and phenylmethanesulfonyl fluoride (PMSF) were obtained from Beyotime Institute of Biotechnology (Jiangsu, China). The Annexin V-FITC Apoptosis Detection Kit was purchased from BestBio Science (Shanghai, China). 20 ng/ml recombinant human bone morphogenetic protein (rhBMP, Bmpr1a agonist) was purchased from PrimeGene Biotechnology (Shanghai, China), and the 30 nM Bmpr1a inhibitor LDN193189 was obtained from MedChemExpress China (Shanghai, China).

Microarray Analysis

The miRNA(GSE36239) and gene expression profile(GSE42177) were downloaded from the public GEO database (www. ncbi.nlm.gov/geo/) [1, 11], The selected array data in GSE36239 dataset consisted of three primary rat cardiomyocytes samples treated with DOX and three controls, and similar design and treatment were given in GSE42177. After data processing as previous [12], differentially expressed miRNAs (DEMs) and differentially expressed genes (DEGs) were identified by significance analysis of the microarrays with the limma package [13], following the criteria $p < 0.05$ and $|\log FC| > 1$.

Gene Ontology (GO) and Pathway Enrichment Analysis of DEGs

GO enrichment analysis of DEGs was implemented with the clusterProfiler package [14]. GO terms (molecular function and biological processes) with adjust p value < 0.05 were considered significantly enriched by DEGs. The clusterProfiler involving Kyoto Encyclopedia of Genes and Genomes (KEGG), Reactome and Molecular Signatures Database (MSigDb) pathway datasets was used to perform pathway enrichment analysis to expound promising signaling pathways correlated with the DEGs, and p value < 0.05 with adjust p value < 0.05 were defined as the cut-off criteria.

Bioinformatics Prediction of miR-15b-5p Targets

First, to list the putative targets of miR-15b-5p, a vast search in mirWalk database (http://zmf.umm.uniheidelberg.de/apps/zmf/mirwalk2/) was performed, in which the miRwalk, miRanda, miRNAMap and Targetscan databases were included. Each target gene must be searched in at least three databases. Commonly, miRNAs negatively regulated the expression of its targets. The candidate targets were narrowed down by an intersection with the DEGs and were further selected by a negative correlation with miR-15b-5p expression.

Cell Culture and Transfection Experiments

The H9c2 cardiomyocytes were obtained from the Shanghai Institutes for Biological Sciences (Shanghai, China), routinely grown in Dulbecco's Modified Eagle (DMEM) medium supplemented with 12% fetal bovine serum in a humidified atmosphere of 5% CO_2 at 37 °C. The cardiomyocytes were exposed to DOX at the concentration of 6 μM for 24 h as previously described [2, 15]. H9c2 cardiomyocytes at 80% confluence were transfected with rno-miR-15-5p mimics (5′-UAGCAGCACAUCAUGGUU UACA-3′) or rno-miR-15-5p inhibitors (5′-UGUAAACCAUGAUGU GCUGCUA-3′), or scrambled controls (Gene Pharma, Shanghai, China), respectively, at a concentration of 20 μM with the use of Lipofectamine 2000(Invitrogen) according to the manufacturer's protocol. All the transfections were performed subsequent to the rhBMP (Bmpr1a agonist) or LDN193189 (Bmpr1a inhibitor) treatment for 30 min.

Apoptosis Assay, Measurement of Mitochondrial Membrane Potential (MMP), and Intracellular ROS

The apoptosis, oxidative stress, and mitochondria damage were common hallmarks of DOX-induced myocardial

damage. To examine the influence of interfering miR-15b-5p or Bmpr1a on apoptosis, MMP and ROS, the experiment was grouped as follows: (1) for interfering miR-15b-5p: control, DOX, DOX + miR-15b-5p mimic (20 μM), DOX + miR-15b-5p inhibitor(20 μM); (2) for interfering Bmpr1a: control, DOX, DOX + rhBMP (20 ng/ml), DOX + LDN193189(30 nM). The H9c2 cardiomyocytes were plated in 6-well culture plates at a density of 5×10^4 cells/mL and then treated with DOX (6 μM) for 24 h followed by apoptosis, MMP and ROS detection according to the manufacturer's protocol. Quantification of apoptotic cells was performed using an Annexin V-FITC/PI Apoptosis Detection kit. MMP changes were detected using the fluorescent probe JC-1(Beyotime, Haimen, China), a lipophilic cationic dye that accumulates in living mitochondria. The intracellular ROS levels were determined using a peroxide-sensitive fluorescent probe (ROS assay kit, DCFH-DA; Beyotime, Haimen, China). The staining protocol detailed for all the samples was performed as previously [16]. The fluorescence was quantificationally analyzed by fluorescence microscopy (Olympus, Tokyo, Japan) and ImageJ software.

Real-time Quantitative PCR (RT-qPCR) Analysis

To examine the regulatory of miR-15b-5p on Bmpr1a signal, the experiment was grouped as follows: control, DOX, DOX + miR-15b-5p mimic, DOX + miR-15b-5p mimic + rhBMP, DOX + miR-15b-5p inhibitor, DOX + miR-15b-5p inhibitor + LDN193189. The mRNA expressions of miR-15b-5p, Bmpr1a, and Gata4 were determined by RT-qPCR. The total miRNA and mRNA samples from H9c2 cardiomyocytes were prepared and detected using the All-in-One™ miRNA RT-qPCR Detection Kit, All-in-OneTM First-Strand cDNA Synthesis Kit and All-in-One™ qPCR Mix (GeneCopoeia, Inc., Rockville, USA) following the manufacturer's protocol. RT-qPCR was carried out with ABI PRISM 7500 instrument (Applied Biosystems, Foster, CA, USA) by implementing SYBR Green according to the manufacturer's instructions. The mRNA and miRNA abundance of each gene was normalized to GAPDH and small nuclear RNA U6, respectively. Relative expression level of genes was calculated with the $2^{-\Delta\Delta Ct}$ method. The validated primers for miR-15b-5p and U6 were purchased from GeneCopoeia, Inc. (Rockville, USA) and GAPDH with other mRNA primers from Sangong Biotech Co., Ltd. (Shanghai, China). The primers for mRNA detections were as follows: rno-Bmpr1a (forward: CAGATTCAGATGGTTCGGCA; reverse: CGCATTAACACCGTCTGGTA), rno-Nkx2-5 (forward:CGCCCCTACATTTTATT CGC; reverse: CAG GTACCGCTGTTGCTTGA), rno-Gata4 (forward: CAC CCCAAT CTCGATATGTTTG; reverse: AGTGTGGTG GTGGTAGTCTG).

Western Blotting Assay

To examine the effect of miR-15b-5p targeting Bmpr1a signal on cell apoptosis and survival of H9c2 cardiomyocytes, the Bcl-2/Bax protein expression ratio (for anti-apoptosis) and Akt activation (for survival) was detected by western blotting, and the experiment was designed as that in the RT-qPCR array. The extraction and detection of cells proteins were performed following standard protocols as described previously [2]. Intensity values of the relative protein levels were normalized to α-Tubulin and analyzed by ImageJ software. For western blotting analysis, the following antibodies were used to recognize the proteins: Akt, p-Akt, Bax, α-Tubulin (Proteintech), Bcl-2 (Affinity Biosciences).

Statistical Analysis

Data are presented as the mean ± standard deviation (SD). Differences between two groups were analyzed using a 2-tailed Student's *t* test and incorporated into GraphPad Prism 7 software (San Diego, CA, USA). One-way analysis of variance (ANOVA) followed by Student–Newman–Keuls test was used when comparing the difference between groups. All the statistical analyses were conducted with SPSS 17.0 software. $p < 0.05$ was considered statistically significant.

Results

miR-15b-5p Expression was Elevated in Cardiomyocytes Treated with DOX

MicroRNA microarray analysis was performed to screen differentially expressed miRNAs (DEMs) by using a public array data (GSE36239), which resulted in 33 DEMs (9 up-regulated and 24 down-regulated) caused by DOX treatment. As shown in Fig. 1a (upper), the heatmap indicated the results of a two-way hierarchical clustering of the samples and the DEMs. Of these DEMs, miR-15b-5p was found increased with a |logFC|=1.11 and $p = 0.001$, which was specially re-illustrated as Fig. 1b. Then, the validation result of RT-qPCR array indicated that DOX significantly up-regulated the expression level of miR-15b-5p by 2.46-fold in H9c2 cells treated with 6 μM for 24 h (Fig. 1c). The target genes of miR-15b-5p were predicted by miRwalk (http://zmf.umm.uniheidelberg.de/apps/zmf/mirwalk2/), miRanda (http://www.microrna.org/microrna/home.do), miRNAMap (http://mirnamap.mbc.nctu.edu.tw/) and Targetscan (http://www.targetscan.org/vert_72/) databases. As

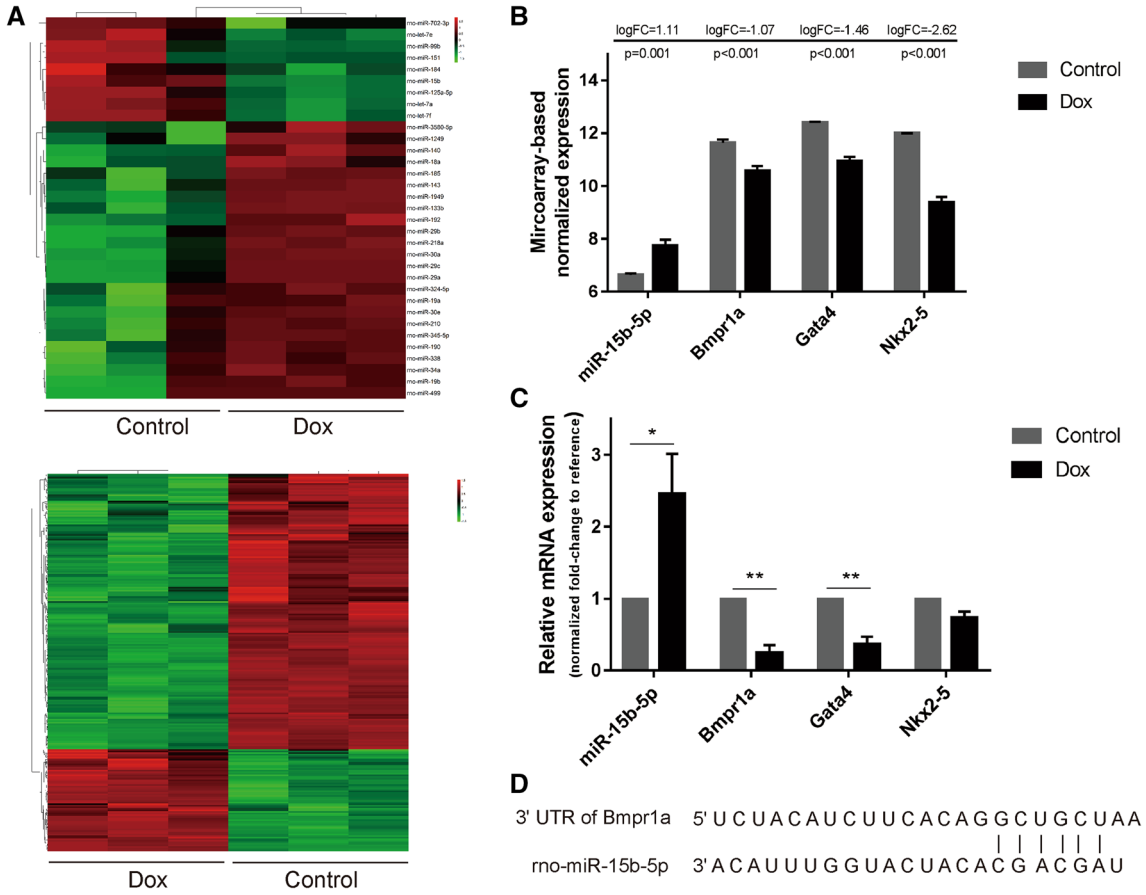

Fig. 1 Assessment of miR-15b-5p and Bmpr1a, Gata4, Nkx2-5 expression upon DOX treatment. **a** the cluster heatmap for the differentially expressed miRNAs (DEMs) and differentially expressed genes (DEGs), which indicated up-regulated with red and down-regulated with green. **b** Microarray-base expressions of miR-15b-5p and Bmpr1a, Gata4, Nkx2-5 were re-illustrated. **c** the mRNA expressions of miR-15b-5p and Bmpr1a, Gata4, Nkx2-5 in H9c2 cardiomyocytes were validated by RT-qPCR. **d** Bmpr1a was predicted as a potential target of miR-15b-5p by bioinformatics databases. Data are represented as mean ± SD ($n=3$); $^{*}p<0.05$, $^{**}p<0.01$

a result, there were 2071 potential target genes listed in at least three databases.

Bmpr1a was Decreased in Cardiomyocytes Treated with DOX and was Considered as a Preferred Target of miR-15b-5p in Combination with the GO and Pathway Enrichments Analyses

The public gene expression profile (GSE42177) was analyzed to explore differentially expressed genes (DEGs) associated with DOX treatment. As displayed in Fig. 1a (lower), 237 DEGs (64 up-regulated and 173 down-regulated) caused by DOX were identified. Of which, some may be the targets of miR-15b-5p. Considering a common negative role of miRNAs in the regulation of target genes, the preferred target may be down-regulated because of that the miR-15b-5p was increased by the DOX treatment. To narrow down the predicted candidate target genes of miR-15b-5p, an intersection between the 173 down-regulated DEGs and the predicted 2071 potential target genes was made, which initially resulted in 27 potential targets. Subsequent to the intersection analysis, we also conducted GO and pathway enrichment analyses to expound the potential biological functions of 237 DEGs and to explore the potential hub target gene. As shown in Table 1, in term of GO enrichment analysis, they were significantly enriched in multiple biological processes related to muscle development, heart development, cardiovascular system development and organ morphogenesis, and enriched in multiple molecular functions related to regulation of phosphate metabolic process, regulation of protein modification process, regulation of protein metabolic process and regulation of protein phosphorylation. In term of pathway enrichment analysis, they were significantly enriched in multiple pathways such as P53 signaling pathway, ALK pathway in cardiomyocytes, regulation of APC activators between G1 S and early anaphase. According to the results of GO and pathway enrichment analyses, ALK pathway may be an important signaling pathway involved

Table 1 Gene ontology(GO) and pathway enrichment analysis of 237 differentially expressed genes identified in GSE42177 dataset

Significant GO terms	Gene list
GO enrichment	
Muscle structure development	ASB2;BHLHE41;CCNB1;DISP1;EGR2;EGR3;FAM65B;FHL2;FZD1;GATA4;GATA6;GDF15;HES1;HEY2;HMGCR;IL6;LIF LMOD2;LRRC10;MYOCD;PKP2;PLPP7;PRICKLE1;PROX1;RARA;RCAN1;SIK1;SPEG;TBX5;USP2;XBP1;ZFPM2
Muscle cell differentiation	ASB2;BHLHE41;CCNB1;FAM65B;FHL2;GATA4;GATA6;GDF15;HES1;HEY2;HMGCR;LMOD2;LRRC10;MYOCD;PLPP7 PRICKLE1;PROX1;RARA;RCAN1;SIK1;SPEG;TBX5;XBP1
Muscle organ development	ASB2;CCNB1;DISP1;EGR2;EGR3;FAM65B;FZD1;GATA6;HEY2;HMGCR;IL6;LIF;MYOCD;PKP2;PRICKLE1;PROX1;RCAN1 SPEG;TBX5;USP2;XBP1;ZFPM2
Muscle tissue development	ASB2;CCNB1;EGR2;FAM65B;FHL2;GATA4;GATA6;HEY2;HMGCR;LRRC10;MYOCD;PKP2;PPARGC1A;PRICKLE1;PROX1 RARA;RCAN1;SIK1;TBX5;USP2;ZFPM2
Heart development	ADRA1A;BMPR1A;CASP3;CCNB1;DLC1;EDNRA;FGF19;FHL2;FZD1;GATA4;GATA5;GATA6;HES1;HEY2;IRX4;JUN;LRRC10 MYOCD;PKP2;PPARA;PRICKLE1;PROX1;RARA;SIK1;SMAD6;SUFU;TAB1;TBX5;ZFPM2
Cardiovascular system development	ADRA1A;BMPR1A;C3AR1;CASP3;CCNB1;CSPG4;CTGF;DHCR7;DLC1;EDNRA;EGR3;EPHA2;FGF18;FGF19;FHL2;FOSL1;FZD1 GATA4;GATA5;GATA6;HES1;HEY2;IL6;IRX4;JUN;LIF;LRRC10;MYOCD;PKP2;PLCD3;PPARA;PRICKLE1;PROX1;RARA;SIK1 SMAD6;SUFU;TAB1;TBX5;XBP1;ZFPM2
Circulatory system development	ADRA1A;BMPR1A;C3AR1;CASP3;CCNB1;CSPG4;CTGF;DHCR7;DLC1;EDNRA;EGR3;EPHA2;FGF18;FGF19;FHL2;FOSL1;FZD1 GATA4;GATA5;GATA6;HES1;HEY2;IL6;IRX4;JUN;LIF;LRRC10;MYOCD;PKP2;PLCD3;PPARA;PRICKLE1;PROX1;RARA;SIK1 SMAD6;SUFU;TAB1;TBX5;XBP1;ZFPM2
Organ morphogenesis	BHLHE41;BMPR1A;CTGF;DLC1;EDNRA;EPHA2;FGD1;FGF18;FHL2;FZD1;GATA4;GATA5;GATA6;HES1;HEY2;IL6;IRX4;JUN KLK4;LIF;PHLDA2;PKP2;PPARA;PPARGC1B;PRICKLE1;PROX1;RARA;SUFU;TAB1;TBX5;TSHR;XBP1;ZFPM2
Regulation of phosphate metabolic process	ACVR1B;ADRA1A;AKAP13;BMPR1A;CASP3;CCNB1;CD80;CDC6;CRY2;CSPG4;CTGF;DLC1;DUSP8;EDNRA;EPHA2;FAM58BP FGF18;FGF19;FLCN;FZD1;GADD45G;GDF15;GRM4;HES1;HMGCR;HSPA2;ICAM1;IL6;JUN;LIF;MAP2K7;MBIP;MLST8;MYOCD NTF3;NUAK1;NUP62;PLK1;PPARA;PPARGC1A;PPARGC1B;PPP2R2B;PPP2
Regulation of phosphorus metabolic process	ACVR1B;ADRA1A;AKAP13;BMPR1A;CASP3;CCNB1;CD80;CDC6;CRY2;CSPG4;CTGF;DLC1;DUSP8;EDNRA;EPHA2;FAM58BP FGF18;FGF19;FLCN;FZD1;GADD45G;GDF15;GRM4;HES1;HMGCR;HSPA2;ICAM1;IL6;JUN;LIF;MAP2K7;MBIP;MLST8;MYOCD NTF3;NUAK1;NUP62;PLK1;PPARA;PPARGC1A;PPARGC1B;PPP2R2B;PPP2
Regulation of protein modification process	ACVR1B;ADRA1A;AKAP13;BMPR1A;BUB1B;CASP3;CCNB1;CD80;CDC20;CDC6;CRY2;CSPG4;CTGF;DLC1;DUSP8;EDNRA EPHA2;FAM58BP;FBXO5;FEM1A;FGF18;FGF19;FLCN;FZD1;FZR1;GADD45G;GDF15;GRM4;HES1;HMGCR;HSPA2;ICAM1;IL6 JUN;LIF;MAP2K7;MBIP;MLST8;MYOCD;NTF3;NUAK1;NUP62;PLK1;PPARGC1
Regulation of cellular protein metabolic process	ACVR1B;ADRA1A;AKAP13;BMPR1A;BUB1B;CASP3;CCNB1;CD80;CDC20;CDC6;CLN8;CRY2;CSPG4;CTGF;DLC1;DUSP8 EDNRA;EPHA2;FAM58BP;FBXO5;FEM1A;FGF18;FGF19;FLCN;FZD1;FZR1;GADD45G;GDF15;GRM4;HES1;HMGCR;HSPA2 ICAM1;IL6;JUN;LIF;MALSU1;MAP2K7;MBIP;MLST8;MYOCD;NTF3;NUAK1;NUP62
Regulation of protein metabolic process	ACVR1B;ADRA1A;AKAP13;BMPR1A;BUB1B;CASP3;CCNB1;CD80;CDC20;CDC6;CLN8;CRY2;CSPG4;CTGF;DLC1;DUSP8 EDNRA;EPHA2;FAM58BP;FBXO5;FEM1A;FGF18;FGF19;FLCN;FZD1;FZR1;GADD45G;GDF15;GRM4;HES1;HMGCR;HSPA2 ICAM1;IL6;JUN;LIF;MALSU1;MAP2K7;MBIP;MLST8;MYOCD;NTF3;NUAK1;NUP62

Table 1 (continued)

Significant GO terms	Gene list
Regulation of phosphorylation	ACVR1B;ADRA1A;AKAP13;BMPR1A;CASP3;CCNB1;CD80;CDC6;CSPG4;CTGF;DUSP8;EDNRA;EPHA2;FAM58BP;FGF18 FGF19;FLCN;FZD1;GADD45G;GDF15;GRM4;HES1;HMGCR;HSPA2;ICAM1;IL6;JUN;LIF;MAP2K7;MBIP;MLST8;MYOCD NTF3;NUP62;PLK1;PPARA;PPARGC1A;PPARGC1B;PROX1;RIPK3;SMAD6;SOCS2;TAB1
Regulation of protein phosphorylation	ACVR1B;ADRA1A;AKAP13;BMPR1A;CASP3;CCNB1;CD80;CDC6;CSPG4;CTGF;DUSP8;EDNRA;EPHA2;FAM58BP;FGF18 FGF19;FLCN;FZD1;GADD45G;GDF15;GRM4;HES1;HMGCR;HSPA2;ICAM1;IL6;JUN;LIF;MAP2K7;MBIP;MLST8;MYOCD NTF3;NUP62;PLK1;PPARGC1A;PROX1;RIPK3;SMAD6;SOCS2;TAB1;TEC;TLR3;TPX2
Significant pathway terms	**Gene list**
Pathway enrichment	
ALK PATHWAY IN CARDIOMYOCYTES	BMPR1A;CHRD;FZD1;GATA4;NKX2-5;SMAD6
P53 SIGNALING PATHWAY	CASP3;CCNB1;GADD45G;PMAIP1;RPRM;STEAP3
REGULATION OF APC ACTIVATORS BETWEEN G1 S AND EARLY ANAPHASE	BUB1B;CCNB1;CDC20;FBXO5;FZR1;PLK1
CELL CYCLE	BUB1B;CCNB1;CDC20;CDC6;FZR1;GADD45G;PLK1
MAPK SIGNALING PATHWAY	CACNB2;CASP3;DUSP8;FGF18;FGF19;GADD45G;HSPA2;JUN;MAP2K7;NTF3;PRKCG;TAB1
TOLL LIKE RECEPTOR SIGNALING PATHWAY	CD80;IL6;JUN;MAP2K7;TAB1;TLR3
TOLL RECEPTOR CASCADES	JUN;MAP2K7;RIPK3;TAB1;TLR3
TOLL LIKE RECEPTOR 3 CASCADE	JUN;MAP2K7;RIPK3;TAB1;TLR3
RHO GTPASE CYCLE	AKAP13;DEPDC7;DLC1;FGD1;RACGAP1;STARD8

in DOX-induced cardiotoxicity. Therefore, we focused on the Bmpr1a which was the main receptor in ALK pathway and the only one of 27 potential targets (Fig. 1d). In the gene microarray analysis, the receptor Bmpr1a in ALK pathway and its downstream transcription factors Gata4 and Nkx2-5 which were specially or highly expressed in cardiac cells were decreased (as shown in Fig. 1b). Then, the down-regulated genes Bmpr1a, Gata4, and Nkx2-5 were further validated by RT-qPCR. As shown in Fig. 1c, DOX markedly decreased the expression levels of Bmpr1a and Gata4 in H9c2 cardiomyocytes ($p < 0.05$) compared to controls, but non-significant for Nkx2-5 ($p > 0.05$).

Interfering miR-15b-5p or Bmpr1a Modulated DOX-Induced Apoptosis, ROS and Mitochondrial Membrane Potential in H9c2 Cardiomyocytes

To examine the role of miR-15b-5p and Bmpr1a in the DOX-induced cardiotoxicity, we detected the apoptosis, ROS and mitochondrial membrane potential by interfering miR-15b-5p or Bmpr1a in H9c2 cardiomyocytes exposed to DOX. As shown in Fig. 2a, after treated with DOX, the early and middle-late apoptosis in H9c2 cardiomyocytes seemed to be increased. However, overexpression of miR-15b-5p by transfecting miR-15b-5p mimic further increased the middle-late apoptosis induced by DOX ($p < 0.01$ vs DOX), while suppression of miR-15b-5p by transfecting miR-15b-5p inhibitor markedly decreased DOX-induced middle-late apoptosis in H9c2 cardiomyocytes ($p < 0.01$ vs DOX), but did not altered the early apoptosis. Meanwhile, stimulating the Bmpr1a signal by rhBMP obviously attenuated the middle-late apoptosis induced by DOX ($p < 0.01$ vs DOX), whereas inhibiting the Bmpr1a signal by BMP inhibitor LDN193189 markedly enhanced the middle-late apoptosis induced by DOX ($p < 0.01$ vs DOX, Fig. 2b). Additionally, we also investigated the influence of interfering miR-15b-5p or Bmpr1a on the ROS of cardiomyocytes exposed to DOX. As shown in Fig. 3a, compared with the control group, DOX significantly promoted ROS production ($p < 0.01$), and the addition of miR-15b-5p mimic significantly enhanced the effect of DOX ($p < 0.05$ vs DOX), while miR-15b-5p inhibitor significantly attenuated the effect of DOX ($p < 0.01$ vs DOX). Simultaneously, the addition of Bmpr1a agonist rhBMP markedly alleviated the effect of DOX ($p < 0.05$ vs DOX), whereas the Bmpr1a inhibitor facilitate the production of ROS induced by DOX ($p < 0.05$ vs DOX, Fig. 3b). Furthermore, the impact of interfering miR-15b-5p or Bmpr1a on the mitochondrial membrane potential (MMP) of H9c2 cells with DOX treatment was evaluated. As shown in Fig. 4a, compared to control group,

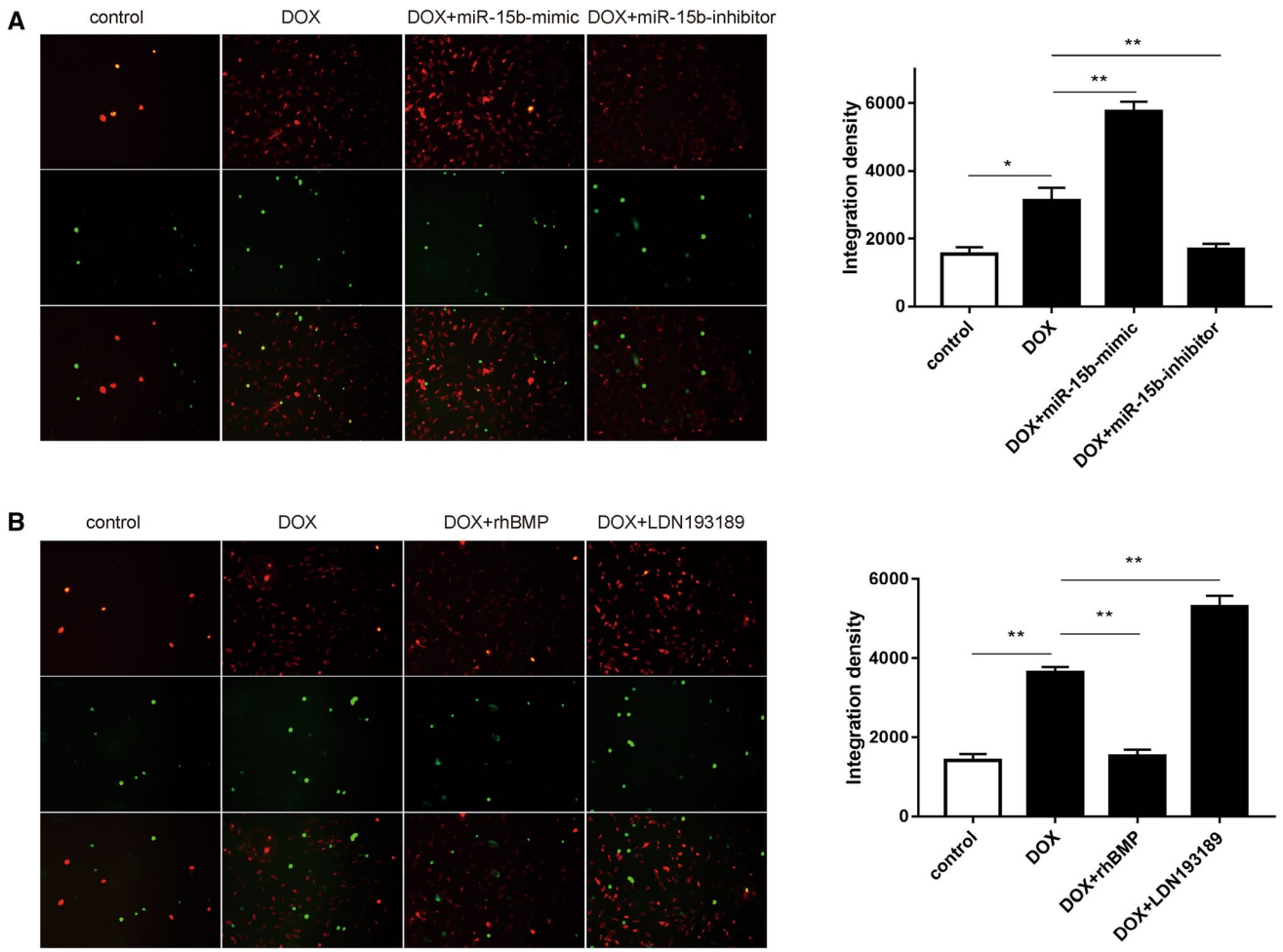

Fig. 2 Effect of interfering miR-15b-5p or Bmpr1a signal on the apoptosis of H9c2 cells treated with DOX. **a** H9c2 cells were treated as following: control, DOX, DOX + miR-15b-mimic and DOX + miR-15b-inhibitor. **b** H9c2 cells were treated as following: control, DOX, DOX + rhBMP (Bmpr1a agonist) and DOX + LDN193189 (Bmpr1a inhibitor). Quantification of apoptotic cells was performed using an Annexin V-FITC/PI Apoptosis Detection kit. The apoptotic cells were indicated by red fluorescence (middle-late apoptosis) and green fluorescence (early apoptosis). The apoptosis was analyzed by fluorescence microscopy and quantified by the red fluorescence plus green fluorescence with ImageJ. Data are represented as mean ± SD ($n = 3$), $^{*}p < 0.05$, $^{**}p < 0.01$

the MMP was impaired with DOX treatment in H9c2 cardiomyocytes ($p < 0.01$), and the impaired MMP was further exacerbated after transfection with miR-15b-5p mimic ($p < 0.05$ vs DOX), but was improved by transfection with miR-15b-5p inhibitor ($p < 0.05$ vs DOX). In the meantime, the use of rhBMP improved the impaired MMP induced by DOX ($p < 0.05$ vs DOX), while the addition of Bmpr1a inhibitor exacerbated the MMP impaired by DOX ($p < 0.01$ vs DOX, Fig. 4b).

miR-15b-5p/Bmpr1a Signaling Regulated the Apoptosis Induced by DOX in H9c2 Cardiomyocytes

Considering the potential role of miR-15b-5p targeting Bmpr1a in DOX-induced cardiotoxicity, we firstly explored the regulatory effect of miR-15b-5p on Bmpr1a signaling. As shown in Fig. 5, the Bmpr1a and Gata4 mRNA were decreased in the cardiomyocytes treated with DOX compared to control group ($p < 0.01$), and they were further reduced by transfection with miR-15b-5p mimic ($p < 0.05$ vs DOX). However, compared to DOX + miR-15b-5p mimic group, the decreased Bmpr1a and Gata4 mRNA were partially rescued by the addition of Bmpr1a agonist rhBMP ($p < 0.05$ vs DOX + miR-15b-5p mimic). In contrast, the decreased Bmpr1a and Gata4 mRNA in the cardiomyocytes treated with DOX was partially restored by transfection with miR-15b-5p inhibitor ($p < 0.05$ vs DOX), while was reduced by the addition of Bmpr1a inhibitor LDN193189 ($p < 0.05$ vs DOX + miR-15b-5p inhibitor, Fig. 5). Then, we explored the effect of interfering miR-15b-5p or Bmpr1a on the expression of proteins related to cell apoptosis and

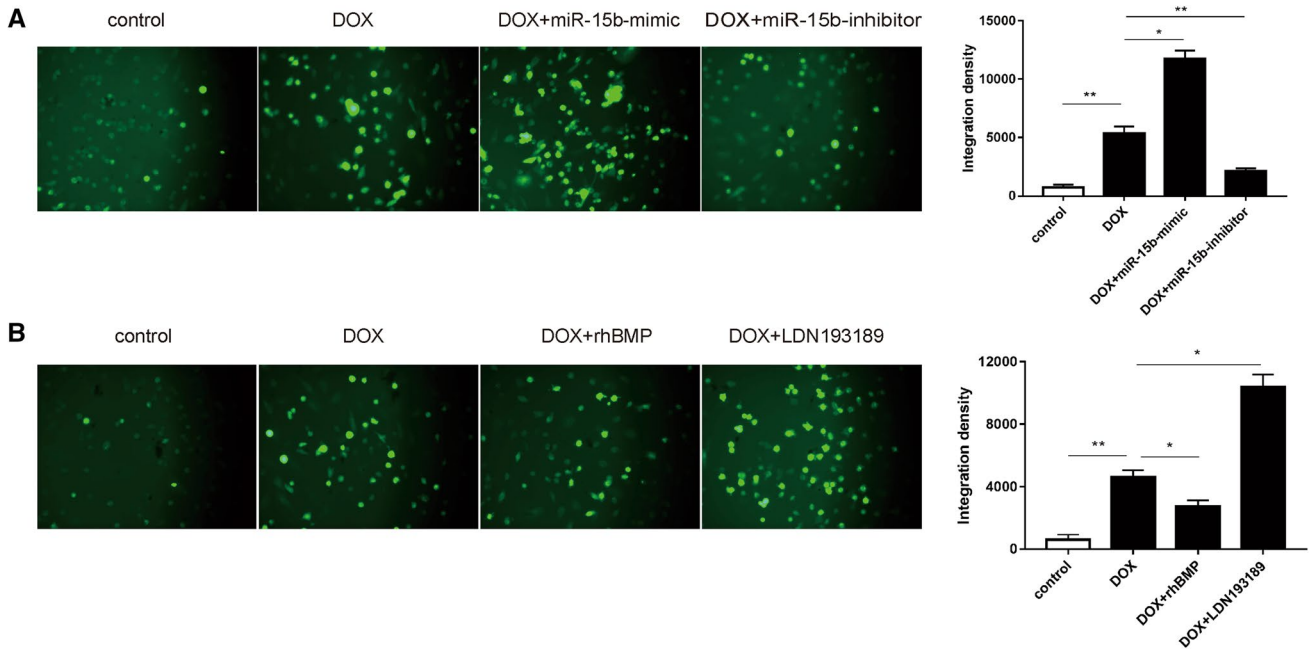

Fig. 3 Effect of interfering miR-15b-5p or Bmpr1a signal on the produced ROS in H9c2 cells treated with DOX. **a** H9c2 cells were treated as following: control, DOX, DOX + miR-15b-mimic and DOX + miR-15b-inhibitor. **b** H9c2 cells were treated as following: control, DOX, DOX + rhBMP (Bmpr1a agonist) and DOX + LDN193189 (Bmpr1a inhibitor). Quantification of ROS was performed using a peroxide-sensitive fluorescent probe (ROS assay kit, DCFH-DA). The ROS was finally analyzed and quantified by fluorescence microscopy and ImageJ. Data are represented as mean ± SD ($n = 3$), *$p < 0.05$, **$p < 0.01$

survival in H9c2 cardiomyocytes. As shown in Fig. 6, compared to control group, the anti-apoptotic capability represented by Bcl-2/Bax ratio was decreased in H9c2 cells with DOX treatment ($p < 0.01$), and the decreased Bcl-2/Bax ratio induced by DOX was further reduced by transfection with miR-15b-5p mimic ($p < 0.01$ vs DOX), which was partially rescued by giving additional Bmpr1a agonist rhBMP ($p < 0.01$ vs DOX + miR-15b-5p mimic). Conversely, the decreased Bcl-2/Bax ratio induced by DOX was partially antagonized by transfection with miR-15b-5p inhibitor ($p < 0.05$ vs DOX), whereas this antagonized effect was subsequently abolished partially by giving additional Bmpr1a inhibitor LDN193189 ($p < 0.05$ vs DOX + miR-15b-5p inhibitor). On the other hand, compared to control group, DOX treatment decreased the survival capability of H9c2 cardiomyocytes ($p < 0.01$, Fig. 6), which was represented by a decreased p-Akt/Akt ratio. The decreased survival capability with decreased p-Akt/Akt ratio caused by DOX was further reduced by transfection with miR-15b-5p mimic ($p < 0.05$ vs DOX), which was partially rescued by giving additional Bmpr1a agonist rhBMP ($p < 0.05$ vs DOX + miR-15b-5p mimic). Simultaneously, the decreased p-Akt/Akt ratio caused by DOX was partially restored by transfection with miR-15b-5p inhibitor ($p < 0.05$ vs DOX), while this effect was partially reversed by giving additional Bmpr1a inhibitor LDN193189 ($p < 0.05$ vs DOX + miR-15b-5p inhibitor). Overall, we demonstrated a role of miR-15b-5p targeting Bmpr1a in DOX-induced cardiotoxicity, and presented the potential importance of miR-15b-5p/Bmpr1a signaling in the regulation of apoptosis induced by DOX in H9c2 cardiomyocytes.

Discussion

Anthracyclines typified by DOX, a well-known commercially available antibiotic antineoplastic agent, have made substantial contribution to the treatment of human malignancies such as leukemia, lymphoma, breast cancer, and solid tumors since late 1960s. This notwithstanding, DOX has attracted much attention not only due to its anti-tumor therapeutic effects with broad spectrum, but also to its serious side effects after long-term use in recent years. The major side effect of DOX is its cumulative and dose-dependent cardiotoxicity, which has seriously restricted its clinical application and benefit. Although efforts have been made to reduce DOX-induced cardiotoxicity underlying the mechanisms aforementioned, encouraging progress has been hampered by the complicated etiology and pathogenesis. The exact mechanisms involved in DOX-induced cardiotoxicity remain largely unknown to date. In the present study, we

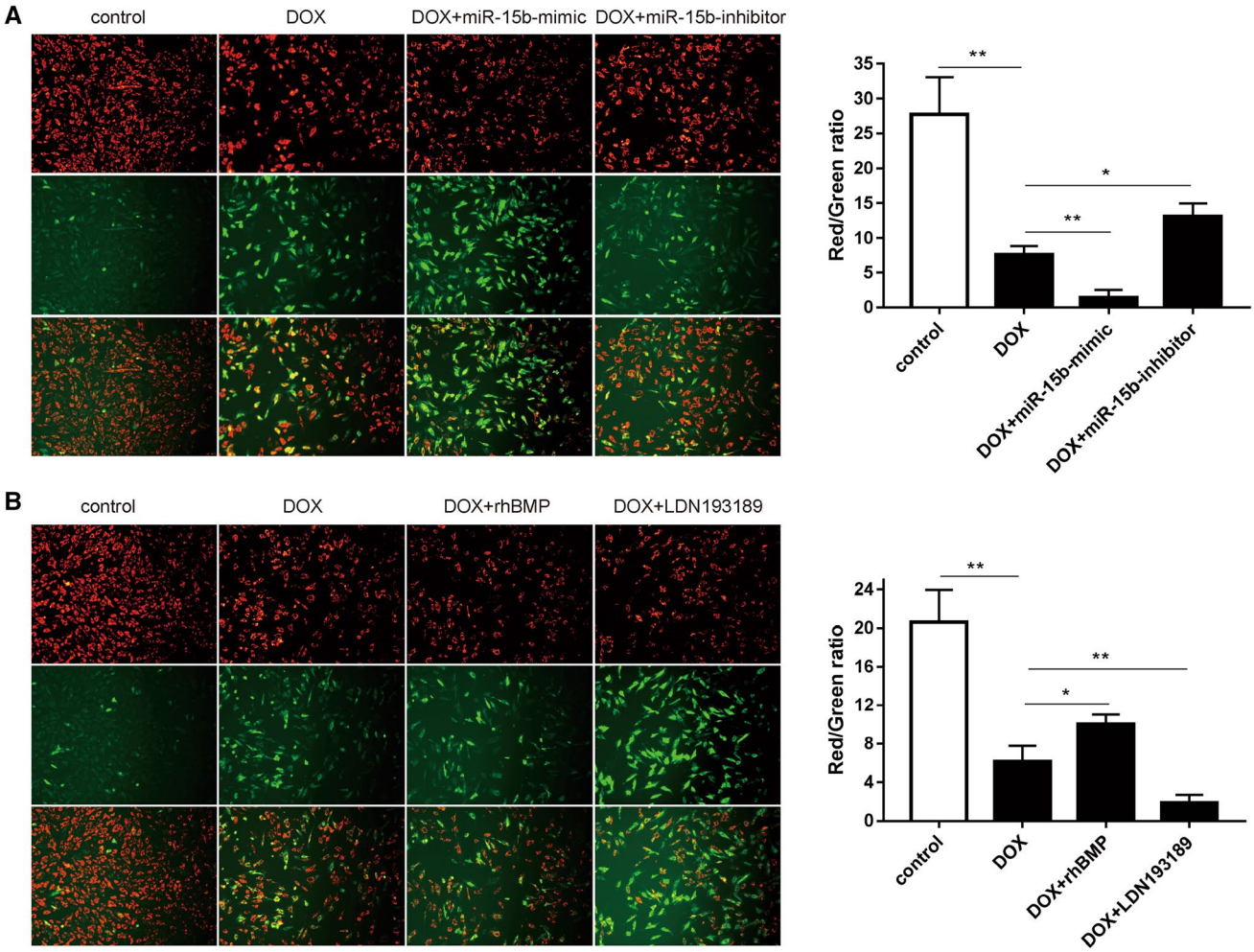

Fig. 4 Effect of interfering miR-15b-5p or Bmpr1a signal on the mitochondrial membrane potential (MMP) in H9c2 cells treated with DOX. **a** H9c2 cells were treated as following: control, DOX, DOX + miR-15b-mimic and DOX + miR-15b- inhibitor. **b** H9c2 cells were treated as following: control, DOX, DOX + rhBMP (Bmpr1a agonist) and DOX + LDN193189 (Bmpr1a inhibitor). Quantification of MMP was performed using a fluorescent probe JC-1. The MMP was analyzed by red and green fluorescence. Cells with red fluorescence indicated favorable MMP while green fluorescence indicated damage. The MMP was finally evaluated by the red/green fluorescence intensity ratio and quantified by ImageJ. Data are represented as mean ± SD ($n = 3$), *$p < 0.05$, **$p < 0.01$

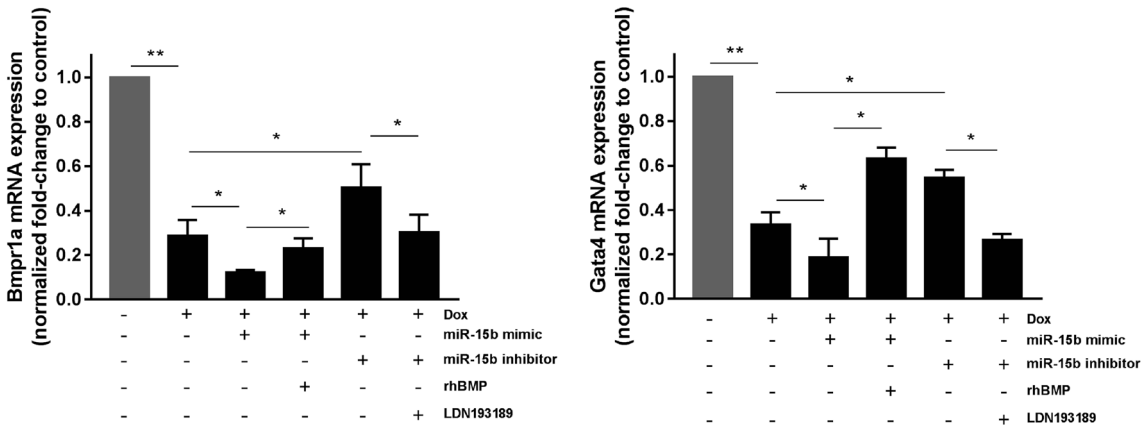

Fig. 5 miR-15b-5p negatively regulated Bmpr1a signal in H9c2 cardiomyocytes. The mRNA expressions of Bmpr1a and Gata4 with different treatments were evaluated by RT-qPCR. Data are represented as mean ± SD ($n = 3$), *$p < 0.05$, **$p < 0.01$

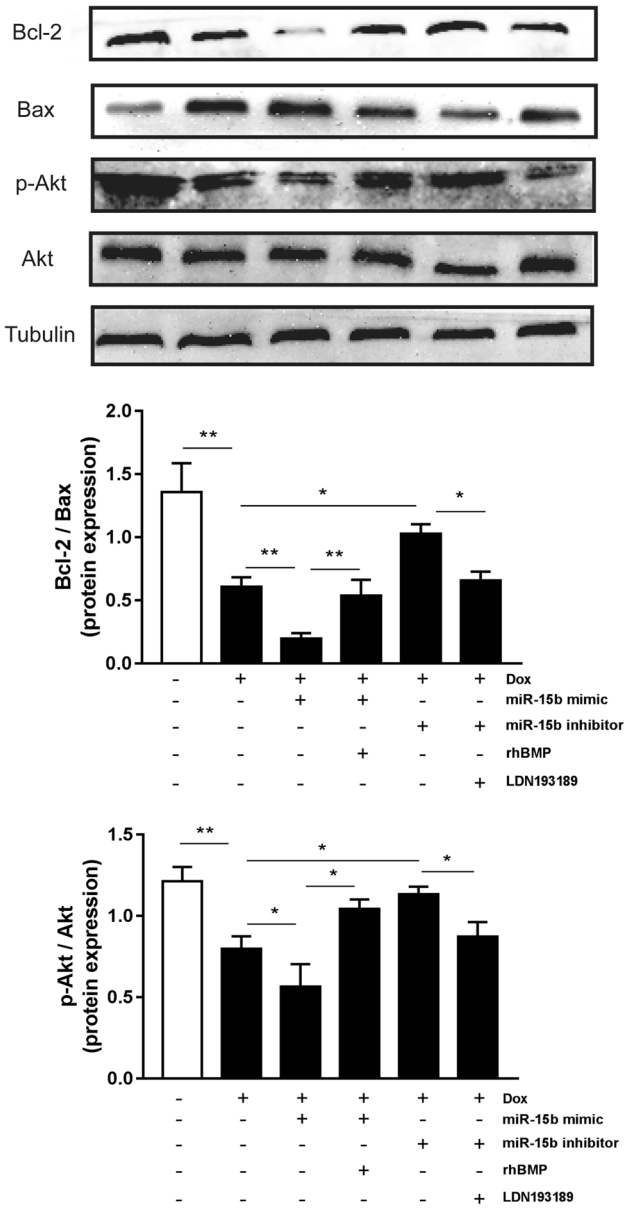

Fig. 6 miR-15b-5p inhibited Bmpr1a signal and correlated with DOX-induced apoptosis in H9c2 cardiomyocytes. The anti-apoptotic capability and Akt activation were evaluated by Bcl-2/Bax and p-Akt/Akt with western blotting. Data are represented as mean ± SD ($n = 3$), $^{*}p < 0.05$, $^{**}p < 0.01$

delineated that DOX-induced cardiotoxicity may be exerted via miR-15b-5p-mediated inhibition of Bmpr1a.

There has been a growing of evidence supporting that miRNAs may server as suitable biomarkers and therapeutic targets for drug-induced cardiotoxicity [17–19]. In the present study, total of 33 differentially expressed miRNAs was initially identified, some of them were reported by the previous studies. In this regard, the role of miR-15b-5p remained undetermined. In this study, the levels of miR-15b-5p were validated to be aberrantly up-regulated in H9c2 cells, suggesting its detrimental role. Previously, miR-15b-5p has also been confirmed to play an accelerative role in hypoxia/reoxygenation- or ischemia reperfusion-induced apoptosis of cardiomyocytes by multiple mechanisms [7, 8]. However, to our knowledge, few studies have concentrated on the role and mechanism of miR-15b-5p in DOX-induced cardiotoxicity except for the study by Holmgren et al. who also supported a potential indicative value of miR-15b-5p in DOX-induced cardiotoxicity [17]. However, only simple screening was conducted in their study. In the current study, our results indicated that reinforced expression of miR-15b-5p may aggravate the DOX-induced apoptosis, oxidative stress and mitochondrial dysfunction, which were common hallmarks of DOX-induced myocardial damage, whereas the suppression of miR-15b-5p could alleviate these effects. In attempt to further uncover the potential mechanism accounting for miR-15b-5p-mediated DOX cardiotoxicity, we employed the public gene microarray data to discovery the possible link between miR-15b-5p and its preferred target based on bioinformatics analysis. Firstly, the GO and pathway enrichment analysis using identified DEGs in cardiomyocytes treated with DOX suggested that DOX exposure might have significant impacts on genes related to heart development and the ALK signaling in cardiomyocytes was likely an important pathway involved in DOX-induced cardiotoxicity. Ultimately as expected, Bmpr1a included in the ALK pathway as a main receptor was indicated as a potential target of miR-15b-5p-mediated DOX cardiotoxicity with the bioinformatics analysis and the observed inverse correlation that an increase in miR-15b-5p expression accompanied with decreased Bmpr1a expression.

Bmpr1a (also known as Alk3), a bone morphogenetic protein receptor activin-like kinase, has been demonstrated required for the development of atrioventricular canal [20]. Previous studies have also reported that Bmpr1a deletion was correlated with congenital heart defects, facial dysmorphism and anomalous growth associated with 10q22q23 deletion syndrome [21], and patchy deletion of Bmpr1a was capable of impairing cardiac contractility [22]. In this study, we have also shown that DOX treatment of cardiac cells leads to the significant down-regulation of Bmpr1a. Molecularly, we also confirmed an attenuated effect of apoptosis, oxidative stress and mitochondrial damage induced by DOX in cardiomyocytes treated with the BMP agonist rhBMP, but enhanced toxic effect with BMP inhibitor. Moreover, we observed the down-regulation of Bmpr1a's downstream transcription factor Gata4 whose preservation has been shown to mitigate doxorubicin-induced myocyte apoptosis and cardiac dysfunction [23]. In this regard, Gata4, a cardiac enriched BMP signal transcription factor, has been documented to up-regulate the expression of several cardiac genes including the antiapoptotic gene Bcl-2 [23, 24]. Collectively, these results suggested, for the first time, a protective role of

Bmpr1a signal in the DOX cardiotoxicity. Actually, the anti-apoptotic capability of Bmpr1a signal has been indicated by the previous studies with the findings that Bmpr1a silencing or knock out could induce the apoptosis of cardiomyocytes [25, 26], while the potentiation of Bmpr1a may accelerate the growth and survival of cardiac cells via the activation of PI3K/Akt pathway mediated by TAK1 [27]. Therefore, it is not surprising that Bmpr1a is accounted as a substantial factor for the maintenance and integrity of cardiac cells. Additionally, to verify the regulatory role of miR-15b-5p on Bmpr1a in DOX cardiotoxicity, interfering of miR-15b-5p or Bmpr1a signal in H9c2 cardiomyocytes exposed to DOX was conducted. As expected, the decreased Bmpr1a and Gata4 mRNA in the cardiomyocytes treated with DOX were partially restored by transfection with miR-15b-5p inhibitor, while was further reduced by miR-15b-5p overexpression or BMP inhibitor LDN193189, suggested a negatively regulatory role of miR-15b-5p on Bmpr1a. In combination with bioinformatics prediction, these results indicated Bmpr1a was potentially a preferred target of miR-15b-5p mediating DOX cardiotoxicity. In the meantime, our results also revealed that interfering of miR-15b-5p or Bmpr1a signal had a significant impact on the Bcl-2/Bax protein expression and activation of Akt signaling, which was consistent with the previous findings [27]. Totally, these results suggested that Bmpr1a was likely a novel indicator for DOX-induced cardiotoxicity and was considered as a preferred target of miR-15b-5p.

Conclusion

In conclusion, the present study provided a novel insight into the pathological mechanisms of DOX-induced cardiotoxicity, and miR-15b-5p/Bmpr1a may be considered as the suitable targets for the treatment of DOX-induced cardiotoxicity.

Compliance with Ethical Standards

Conflict of interest The authors declare that they have no conflict of interest with respect to the research, authorship, and/or publication of this article.

References

1. Roca-Alonso, L., Castellano, L., Mills, A., Dabrowska, A. F., Sikkel, M. B., Pellegrino, L.,et al (2015). Myocardial MiR-30 downregulation triggered by doxorubicin drives alterations in beta-adrenergic signaling and enhances apoptosis. *Cell Death & Disease, 6*, e1754.
2. Zhao, L., Qi, Y., Xu, L., Tao, X., Han, X., Yin, L.,et al (2018). MicroRNA-140-5p aggravates doxorubicin-induced cardiotoxicity by promoting myocardial oxidative stress Via targeting Nrf2 and Sirt2. *Redox Biology, 15*, 284–296.
3. Mukhopadhyay, P., Rajesh, M., Batkai, S., Kashiwaya, Y., Hasko, G., Liaudet, L.,et al (2009). Role of superoxide, nitric oxide, and peroxynitrite in doxorubicin-induced cell death in vivo and in vitro. *American Journal of Physiology Heart and Circulatory Physiology, 296*, H1466–H1483.
4. Zhang, S., Liu, X., Bawa-Khalfe, T., Lu, L. S., Lyu, Y. L., Liu, L. F.,et al (2012). Identification of the molecular basis of doxorubicin-induced cardiotoxicity. *Nature Medicine, 18*, 1639–1642.
5. Pecoraro, M., Del, P. M., Marzocco, S., Sorrentino, R., Ciccarelli, M., Iaccarino, G.,et al (2016). Inflammatory Mediators in a short-time mouse model of doxorubicin-induced cardiotoxicity. *Toxicology and Applied Pharmacology, 293*, 44–52.
6. Wang, J. X., Zhang, X. J., Feng, C., Sun, T., Wang, K., Wang, Y.,et al (2015). MicroRNA-532-3p regulates mitochondrial fission through targeting apoptosis repressor with caspase recruitment domain in doxorubicin cardiotoxicity. *Cell Death & Disease, 6*, e1677.
7. Liu, L. F., Liang, Z., Lv, Z. R., Liu, X. H., Bai, J., Chen, J.,et al (2012). MicroRNA-15a/b are up-regulated in response to myocardial ischemia/reperfusion injury. *Journal of Geriatric Cardiology, 9*, 28–32.
8. Liu, L., Zhang, G., Liang, Z., Liu, X., Li, T., Fan, J.,et al (2014). MicroRNA-15b enhances hypoxia/reoxygenation-induced apoptosis of cardiomyocytes via a mitochondrial apoptotic pathway. *Apoptosis, 19*, 19–29.
9. Roy, S., Banerjee, J., Gnyawali, S. C., Khanna, S., He, G., Pfeiffer, D.,et al (2013). Suppression of induced microrna-15b prevents rapid loss of cardiac function in a dicer depleted model of cardiac dysfunction. *PLoS ONE, 8*, e66789.
10. Nishi, H., Ono, K., Iwanaga, Y., Horie, T., Nagao, K., Takemura, G.,et al (2010). MicroRNA-15b modulates cellular ATP levels and degenerates mitochondria via Arl2 in neonatal rat cardiac myocytes. *Journal of Biological Chemistry, 285*, 4920–4930.
11. Jain, S., Wei, J., Mitrani, L. R., & Bishopric, N. H. (2012). Autoacetylation stabilizes P300 in cardiac myocytes during acute oxidative stress, promoting STAT3 accumulation and cell survival. *Breast Cancer Research and Treat, 135*, 103–114.
12. Wan, G., Ji, L., Xia, W., Cheng, L., & Zhang, Y. (2018). Screening genes associated with elevated neutrophiltolymphocyte ratio in chronic heart failure. *Molecular Medicine Reports, 18*, 1415–1422.
13. Ritchie, M. E., Phipson, B., Wu, D., Hu, Y., Law, C. W., Shi, W.,et al (2015). Limma powers differential expression analyses for RNA-sequencing and microarray studies. *Nucleic Acids Research, 43*, e47.
14. Yu, G., Wang, L. G., Han, Y., & He, Q. Y. (2012). ClusterProfiler: An R Package for comparing biological themes among gene clusters. *Omics-A Journal of Integrative Biology, 16*, 284–287.
15. Zhao, L., Tao, X., Qi, Y., Xu, L., Yin, L., & Peng, J. (2018). Protective effect of dioscin against doxorubicin-induced cardiotoxicity via adjusting microRNA-140-5p-mediated myocardial oxidative stress. *Redox Biology, 16*, 189–198.
16. Zhang, A., Sheng, Y., & Zou, M. (2017). Antiproliferative activity of alisol B in MDA-MB-231 cells is mediated by apoptosis, dysregulation of mitochondrial functions, cell cycle arrest and generation of reactive oxygen species. *Biomedicine & Pharmacotherapy, 87*, 110–117.
17. Holmgren, G., Synnergren, J., Andersson, C. X., Lindahl, A., & Sartipy, P. (2016). MicroRNAs as potential biomarkers for doxorubicin-induced cardiotoxicity. *Toxicology in Vitro, 34*, 26–34.
18. Chaudhari, U., Nemade, H., Gaspar, J. A., Hescheler, J., Hengstler, J. G., & Sachinidis, A. (2016). MicroRNAs as early toxicity signatures of doxorubicin in human-induced pluripotent stem cell-derived cardiomyocytes. *Archives of Toxicology, 90*, 3087–3098.
19. Ruggeri, C., Gioffre, S., Achilli, F., Colombo, G. I., & D'Alessandra, Y. (2018). Role of microRNAs in

doxorubicin-induced cardiotoxicity: An overview of preclinical models and cancer patients. *Heart Failure Reviews, 23*, 109–122.
20. Gaussin, V., Morley, G. E., Cox, L., Zwijsen, A., Vance, K. M., Emile, L.,et al (2005). Alk3/Bmpr1a receptor is required for development of the atrioventricular canal into valves and annulus fibrosus. *Circulation Research, 97*, 219–226.
21. Breckpot, J., Tranchevent, L. C., Thienpont, B., Bauters, M., Troost, E., Gewillig, M.,et al (2012). BMPR1A is a candidate gene for congenital heart defects associated with the recurrent 10Q22q23 deletion syndrome. *European Journal of Medical Genetics, 55*, 12–16.
22. El-Bizri, N., Wang, L., Merklinger, S. L., Guignabert, C., Desai, T., Urashima, T.,et al (2008). Smooth muscle protein 22Alpha-mediated patchy deletion of Bmpr1a impairs cardiac contractility but protects against pulmonary vascular remodeling. *Circulation Research, 102*, 380–388.
23. Kobayashi, S., Volden, P., Timm, D., Mao, K., Xu, X., & Liang, Q. (2010). Transcription factor GATA4 inhibits doxorubicin-induced autophagy and cardiomyocyte death. *Journal of Biological Chemistry, 285*, 793–804.
24. Kobayashi, S., Lackey, T., Huang, Y., Bisping, E., Pu, W. T., Boxer, L. M.,et al (2006). Transcription factor Gata4 regulates cardiac BCL2 gene expression in vitro and in vivo. *Faseb Journal, 20*, 800–802.
25. Wu, Y., Zhou, X., Huang, X., Xia, Q., Chen, Z., Zhang, X.,et al (2016). Pax8 plays a pivotal role in regulation of cardiomyocyte growth and senescence. *Journal of Cellular and Molecular Medicine, 20*, 644–654.
26. Yang, D., Lai, D., Huang, X., Shi, X., Gao, Z., Huang, F.,et al (2012). The defects in development and apoptosis of cardiomyocytes in mice lacking the transcriptional factor Pax-8. *International Journal of Cardiology, 154*, 43–51.
27. Sui, X., Li, D., Qiu, H., Gaussin, V., & Depre, C. (2009). Activation of the bone morphogenetic protein receptor by H11kinase/Hsp22 promotes cardiac cell growth and survival. *Circulation Research, 104*, 887–895.